International Journal of Thermophysics, Vol. 1, No. 2, 1980

A Transient (Subsecond) Technique for Measuring Heat of Fusion of Metals

A. Cezairliyan[1] and A. P. Miiller[1]

Received December 20, 1979

A transient technique is described for measuring the heats of fusion of metals with melting temperatures above 1500 K. The specimen configuration consists of a strip of the metal under study "sandwiched" between two strips of another metal with a higher melting temperature. The basic method consists of rapidly heating the composite specimen by passing a subsecond-duration electrical current pulse through it and simultaneously measuring the radiance temperature of the containment metal surface, as well as the current through and voltage drop across the specimen. The melting of the metal under study is manifested by a plateau in the temperature versus time function for the containing metal surface. The time integral of the power absorbed by the specimen during melting yields the heat of fusion. Measurements on several tantalum–niobium–tantalum specimens yield a value of 31.5 $kJ \cdot mol^{-1}$ for the heat of fusion of niobium, with an estimated maximum inaccuracy of ± 5%.

KEY WORDS: dynamic techniques; heat of fusion; high temperatures; melting; niobium.

1. INTRODUCTION

The measurements of thermophysical properties of refractory metals around their melting points present several technical problems that rapidly become more severe with increasing temperature and duration of the experiment. Some of the difficulties arise from heat losses, evaporation, and chemical reaction, which become major problems when dealing with liquid metals at high temperatures.

[1]Thermophysics Division, National Bureau of Standards, Washington, D.C. 20234, USA.

0195-928X/80/0600-0195$03.00/0

The problem of chemical reaction has been partially solved by the technique of electromagnetic levitation combined with drop calorimetry [1, 2], making it possible to measure enthalpy of liquid as well as solid specimens. However, severe radiative heat losses above 3000 K and the high vapor pressure of liquid metals limit the temperature range of this relatively slow (~ seconds to minutes) technique.

The aforementioned problems are reduced significantly through the use of various pulse heating techniques. These can be classified according to duration of the experiment: subsecond (heating rates $\sim 10^4$ K · s^{-1}) and submillisecond (heating rates $\sim 10^8$ K · s^{-1}). The submillisecond pulse methods [3, 4] (often referred to as capacitor discharge methods) are particularly applicable to the study of liquid metals, since radiative heat losses are relatively small until very high temperatures. However, at these high speeds, the measurements of experimental quantities present difficulties and are inherently less accurate than those in slower transient techniques [5, 6].

The subsecond pulse heating technique developed at the National Bureau of Standards [5, 6] has been successfully used for measurements of thermal and electrical properties of a number of electrically conducting refractory materials. These experiments were essentially limited to the solid phase, since the measurement times were longer than the hydrodynamic collapse times of the specimens in their liquid phase. In this paper, the temperature range of the pulse heating system at NBS has been extended somewhat above melting temperatures for the purpose of measuring the heats of fusion of refractory metals.

The specimen configuration consists of a strip of the metal under study "sandwiched" between two strips of another metal with a higher melting temperature. The method involves measuring the radiance temperature[2] of the containment metal as well as the current through and voltage drop across the composite specimen as it undergoes rapid resistive self-heating from room temperature to high temperatures (above 1500 K) in less than 1 s. The experimental quantities are recorded digitally every 0.4 ms with a full-scale resolution of about 1 part in 8000. The melting of the metal under study is manifested by a plateau in the temperature versus time function for the containing metal surface. The heat of fusion is determined from the time integral of the power absorbed by the specimen during the melting period. Details regarding the construction and operation of the measurement system, the methods of measuring experimental quantities, and other pertinent information is given elsewhere [5, 6].

For the present feasibility study, we have selected niobium as the

[2]Radiance temperature (sometimes referred to as brightness temperature) of the specimen surface is the temperature at which a blackbody has the same radiance as the surface, corresponding to the effective wavelength of the measuring pyrometer. See also, Eq. (3).

lower-melting material, with tantalum as the higher-melting material, on the basis of their compatibility from a resistivity point of view, as well as other favorable high-temperature properties (such as heat capacity and thermal expansion) in the solid phase. In addition, niobium was selected because of the disagreement that exists in the literature among values reported for its heat of fusion.

2. MEASUREMENTS

The composite specimens were constructed from niobium and tantalum strips of the following nominal dimensions: length, 75 mm; width, 6 mm; thickness, 0.13–0.38 mm (0.005–0.015 in.). The strips were clamped together in the configuration illustrated in Fig. 1. In addition, the clamped strips were spot-welded at several locations along their length to ensure good thermal contact at the tantalum–niobium interfaces. Four thickness combinations of Ta–Nb–Ta specimens were fabricated in order to elucidate any problems arising from temperature gradients and/or chemical reaction during the experiments. The four groups are conveniently labeled throughout this paper according to the thickness combinations in units of 10^{-3} in., 5-10-5, 5-15-5,

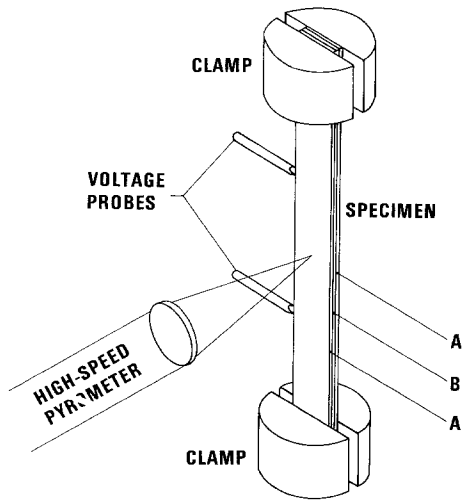

Fig. 1. Schematic diagram showing the arrangement of the composite specimen, clamps, voltage probes, and the radiance temperature measurement system. A strip of the metal under study (B) is clamped between two strips of another metal (A) with a higher melting temperature. The composite specimen is nominally 75 mm in length by 6 mm in width.

10-10-10 and 10-15-10. In addition, two groups of Ta–Ta–Ta specimens (5-10-5 and 10-10-10) were also fabricated for measurements of the hemispherical total emittance of the tantalum-5 and tantalum-10 surfaces.

A summary of the properties of the composite specimens is given in Table I. Table II presents the results of the impurity analyses typical of the niobium and tantalum material as reported by the manufacturer; both materials appear to be about 99.9% pure or better. The temperature range of the high-speed pyrometer [7] was selected so that in all experiments the melting plateau appeared about midrange; in this way, data were obtained continuously before, during, and after melting of a composite specimen in a single pulse heating experiment.

Prior to each experiment, we adjusted a resistance in series with the specimen and/or the voltage of the battery bank in order to achieve the desired heating rate. The specimen was then heated in an argon environment

Table I. Properties of the Ta–Nb–Ta Composite Specimens Used in Determining the Heat of Fusion and Electrical Resistivity of Nb

Property	Unit	Tantalum	Niobium
Atomic mass	$g \cdot mol^{-1}$	180.95	92.91
Density	$g \cdot cm^{-3}$	16.6	8.57
Melting temperature[a]	K		2750
Heat capacity[b]	$J \cdot mol^{-1} \cdot K^{-1}$	$C_p = A + BT + T^2 + DT^3$ where $A = -6.549$, $B = 4.583 \times 10^{-2}$, $C = -2.013 \times 10^{-5}$, $D = 3.325 \times 10^{-9}$, $1900 < T < 3000$ K	
Electrical resistivity[b]	$\mu\Omega \cdot cm$	$\rho = A + BT + CT^2$ where $A = 3.671$, $B = 4.292 \times 10^{-2}$, $C = -2.677 \times 10^{-6}$, $1900 < T < 3000$ K	
Geometry		Thin rectangular strips	Thin rectangular strips
Nominal dimensions			
Total length	mm	75	75
Effective length[c]	mm	25	25
Width	mm	6	6
Thickness	mm	0.13–0.25	0.25–0.38
Thickness	10^{-3} in	5–10	10–15
Purity	% by mass	99.9+	99.9

[a]Melting temperature of Nb as measured by Cezairliyan [9].
[b]Heat capacity and electrical resistivity of Ta as measured by Cezairliyan et al. [11].
[c]Effective refers to the portion of the specimen between the voltage probes.

Table II. Impurities in the Specimen Materials According to the Manufacturer's Analyses

Specimen material	Detected impurities in ppm by mass										
	Nb	Ta	W	Zr	Mo	Hf	Fe	C	O	N	Total all other
Nb	Major	430	<100	<200	<100	<100	<50	14	74	51	<270[a]
Ta	140	Major	170	<10	<10		75	<10	53	28	<130[b]

[a]Each of the other detected elements is less than 20 ppm.
[b]Each of the other detected elements is less than 10 ppm.

at atmospheric pressure from room temperature to the desired temperature by means of an electrical current pulse of about 400–750 ms duration. Heating rates were varied between approximately 3700 and 8500 $K \cdot s^{-1}$ for the different specimens. Upon completion of the experiments, we calibrated the pyrometer, using a tungsten filament reference lamp which, in turn, had

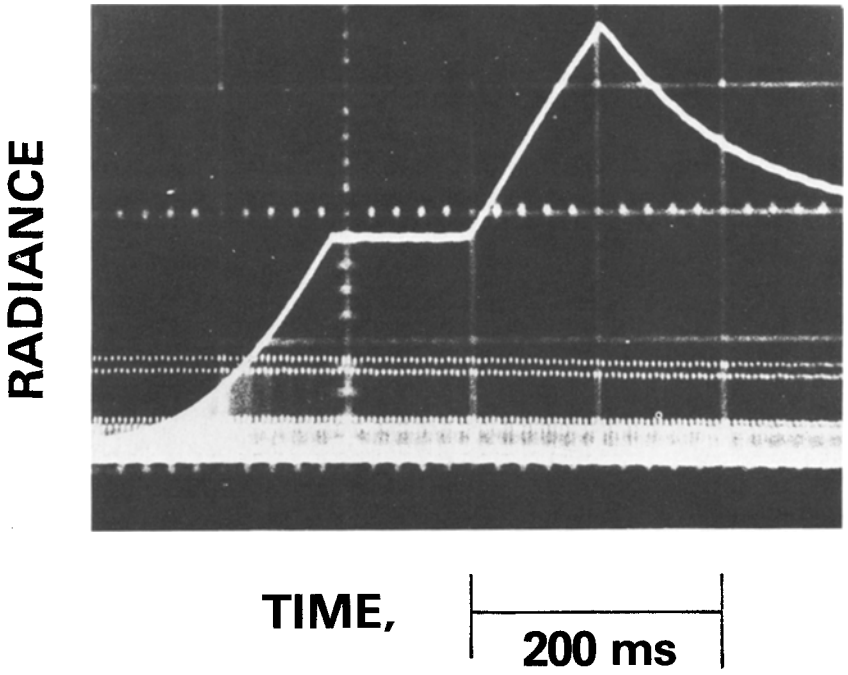

Fig. 2. Oscilloscope trace photograph of the specimen radiance (as observed by the pyrometer) during a typical pulse heating experiment. Dots forming the horizontal lines in the pyrometer output correspond to the radiance from a reference source.

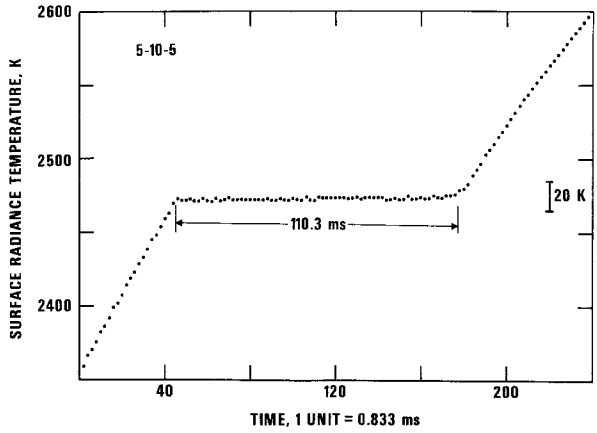

Fig. 3. Variation of radiance temperature as a function of time near and at the melting temperature of niobium (Ta–Nb–Ta specimen with a relative thickness of 5-10-5). The points represent temperatures obtained from individual pyrometer readings.

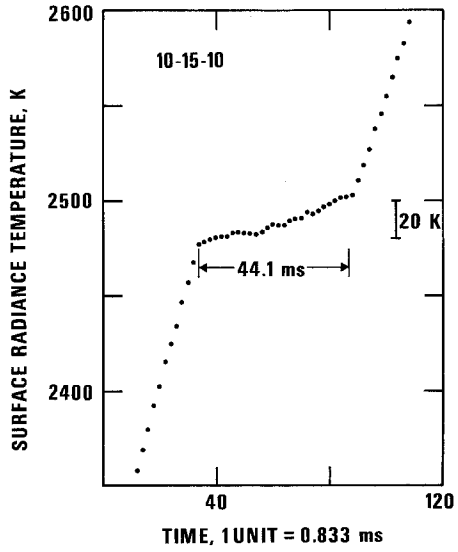

Fig. 4. Variation of radiance temperature as a function of time near and at the melting temperature of niobium (Ta–Nb–Ta specimen with a relative thickness of 10-15-10). The diagram illustrates the effect of using an extremely high energy input rate.

been calibrated against the National Bureau of Standards Photoelectric Pyrometer by the Radiometric Physics Division at NBS.

An oscilloscope trace photograph showing the time variation of the specimen surface radiance, as seen by the pyrometer during a typical pulse heating experiment, is presented in Fig. 2. The plateau in the heating curve indicates the solid-to-liquid transformation of niobium. Figure 3 shows the variation of radiance temperature for a composite specimen as a function of time near and during the transformation; in this experiment, the rate of energy absorption by the niobium during melting was 291 kJ · mol^{-1} · s^{-1}. It is interesting to compare these data with those illustrated in Fig. 4, where melting has occurred at an energy input rate of 720 kJ · mol^{-1} · s^{-1}. Experiments involving very high energy input rates often resulted in poorly formed melting plateaus, as in Fig. 4; in such cases, the data were not used in determining the heat of fusion.

Photomicrographs of a 5-15-5 and a 10-15-10 specimen, taken after the

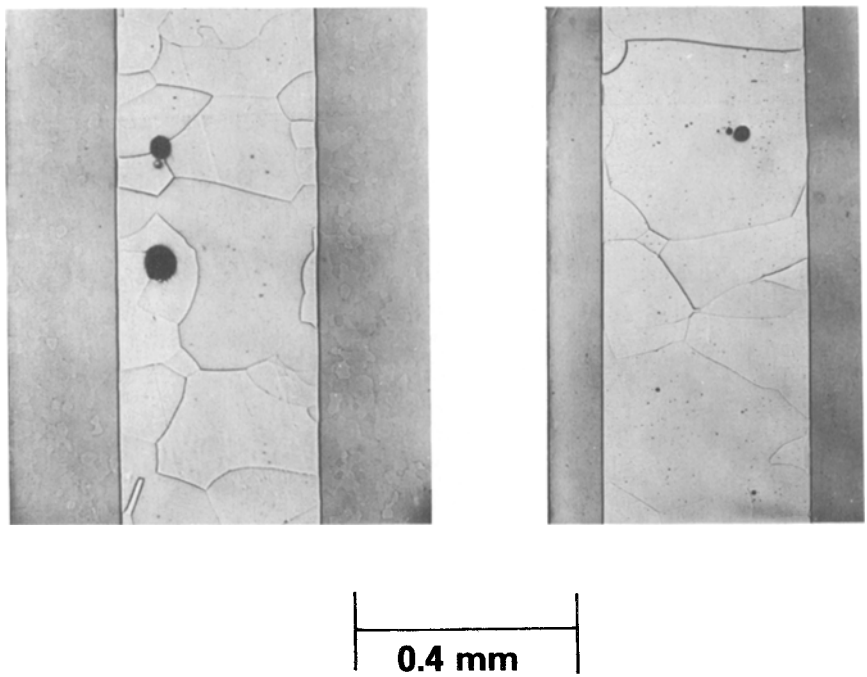

Fig. 5. Photomicrographs of a 10-15-10 (left) and a 5-15-5 (right) Ta–Nb–Ta specimen sectioned lengthwise after experiments in which each specimen was rapidly heated through the solid–liquid transformation point of niobium.

melting experiments, are shown in Fig. 5. Considerable grain growth appears to have taken place as a result of melting followed by rapid solidification. Some spherical voids arising from gaseous impurities are also visible.

3. RESULTS

The heat of fusion was determined from a consideration of the power balance during the heating period of the experiment. The instantaneous power absorbed by metal B in an A-B-A composite specimen is given by

$$P_{\mathrm{B}} = P_i - P_r - P_{\mathrm{A}} \tag{1}$$

where P_i is the power imparted to the effective specimen, P_r is the power radiated by the effective specimen surface, and P_{A} is the power absorbed by the containment metal A as manifested by a rise in its temperature. Power losses arising from conduction through the ends of the effective specimen were considered negligible under the operational conditions of our experiments [5]. Therefore, the heat of fusion of material B is obtained from the time integral of the power absorbed by B during the melting period:

$$Q_f = \frac{1}{n_B} \int_{t_1}^{t_2} (P_i - P_r - P_A)\, dt \tag{2}$$

where n_{B} is the number of moles of metal B contained in the effective specimen, and t_1 and t_2 are the times corresponding to the beginning and the end of the melting period, respectively.

The leading term in Eq. (2), that is, the time integral of $P_i = EI$, where E is the potential difference across the effective specimen, and I is the current through the specimen, yields the energy imparted to the specimen during melting, W_i. It is important to note that the computation of W_i involves the temperature only insofar as the measured temperature-time function is used to determine the duration of the melting period. Therefore, the values of W_i are not affected significantly by systematic errors that might arise in determining the specimen temperature.

The second and third terms in Eq. (2), involving time integrals of P_r and P_{A}, are the heat loss corrections that must be applied to W_i in order to obtain the heat of fusion. Since P_r and P_{A} are both explicit functions of true temperature (see below), it is necessary to convert the measured radiance temperatures into true temperatures before any heat loss corrections are evaluated.

All temperatures reported in this work are based on the International

Practical Temperature Scale of 1968 [8]. In all computations, the geometrical quantities are based on their room temperature dimensions.

3.1. True Temperature Determination

The true temperature and the radiance temperature can be related to each other through the defining equation for normal spectral emittance:

$$\epsilon_\lambda = \frac{i_\lambda(T)}{i_{\lambda b}(T)} = \frac{i_{\lambda b}(T_R)}{i_{\lambda b}(T)} \tag{3}$$

where ϵ_λ is the normal spectral emittance, i_λ is the normal spectral radiance, b denotes a blackbody, T is the true temperature, and T_R is the radiance temperature. Substituting the exact (Planck) expression for i_λ, then making the Wien approximation,

$$\epsilon_\lambda = \frac{\exp\left[c_2/\lambda T\right] - 1}{\exp\left[c_2/\lambda T_R\right] - 1} \simeq \frac{\exp\left[c_2/\lambda T\right]}{\exp\left[c_2/\lambda T_R\right]} \tag{4}$$

or, rearranging terms,

$$\frac{1}{T} - \frac{1}{T_R} \simeq \frac{\lambda \ln \epsilon_\lambda}{c_2} \tag{5}$$

This approximation, from which we calculated true temperatures, introduces in our temperature range an error into the calculation of T from a given T_R not exceeding 0.06 K. The radiance measurements were performed at 653 nm, the effective wavelength of the pyrometer's interference filter; the bandwidth of the filter was 10 nm. The circular area viewed by the pyrometer was 0.2 mm in diameter.

For each specimen, we fitted the measured radiance temperatures for the premelting and melting periods by the least-squares method, with a quadratic and a linear function of time, respectively; the radiance temperature at the intersection of the two functions was taken as the radiance temperature of the tantalum surface at the beginning of the niobium melting period. The resulting temperatures are given in Table III. The temperatures are also plotted in Fig. 6 as a function of heating rate (evaluated at 20 K below the melting plateau). It can be seen that changes in the heating rate do not seem to affect the radiance temperature significantly. However, the temperatures for the 5-10-5 and 5-15-5 specimens are on the average about 5 K lower than those for the 10-10-10 and 10-15-10 specimens. This difference may arise from temperature gradients within the tantalum

Table III. Results on the Determination of Radiance Temperature of the Ta–Nb–Ta Composite Specimens at 2750 K

Specimen number	Relative thickness[a] Ta–Nb–Ta	Premelting period: Heating rate[b] (K · s^{-1})	Premelting period: Std. Dev.[c] (K)	Slope of melting plateau[d] (K · s^{-1})	Radiance temp. of Ta at melting Temp. of Nb[g]: Temp.[e] (K)	Radiance temp. of Ta at melting Temp. of Nb[g]: Std. dev.[f] (K)	Normal spectral emittance of Ta at melt. temp. of Nb[g]
1	5-10-5	3710	1.0	11	2471.8	0.6	0.406
2	5-10-5	3740	1.1	25	2471.4	0.8	0.405
3	5-15-5	4450	1.2	17	2470.6	0.7	0.404
4	5-15-5	4010	1.2	29	2469.6	0.8	0.403
5	5-15-5	5150	1.4	22	2469.4	1.0	0.402
6	5-15-5	8450	1.6	91	2471.8	0.7	0.406
7	10-10-10	4570	1.0	172	2476.5	0.9	0.413
8	10-15-10	4650	1.3	166	2476.7	0.9	0.413
9	10-15-10	4700	1.2	185	2474.4	0.8	0.410

[a]Also indicates the nominal thicknesses in units of 10^{-3} in for Ta and Nb strips used in the composite specimens.

[b]Evaluated at approximately 20 K below the melting temperature of niobium.

[c]Represents the standard deviation of an individual temperature from the smooth temperature versus time function (quadratic) obtained by the least-squares method.

[d]Slope of the linear fit to the melting plateau obtained by the least-squares method.

[e]The temperature defined by the intersection of two functions, each of which were derived from least-squares fits to the radiance temperature versus time data prior to melting (quadratic function) and on the melting plateau (linear function).

[f]Represents the standard deviation of an individual temperature from the smooth temperature versus time function (linear) obtained by the least-squares method.

[g]2750 ± 10 K [9].

containment strip or from lower emissivity of the tantalum-5 surfaces, as suggested by the measurements of hemispherical total emittance described below, or from both.

The value of ϵ_λ for tantalum at the true melting temperature of niobium, taken as 2750 ± 10 K[9], was determined for each specimen from the measured radiance temperature at this melting temperature by means of Eq. (5); the results are given in Table III. The average value of ϵ_λ for the tantalum-5 surfaces at 2750 K is approximately 0.404, which is about 2% lower than the corresponding average of 0.412 for the tantalum-10 surfaces.

For radiance temperatures between 2400 and 2900 K, the variation of ϵ_λ for each tantalum surface was represented by a separate quadratic function in radiance temperature based on the value of ϵ_λ at the radiance temperature corresponding to 2750 K for a given specimen and the slope of the ϵ_λ data of

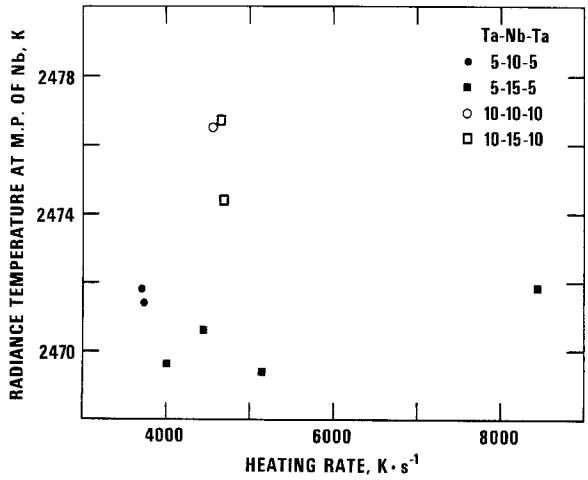

Fig. 6. Radiance temperatures of the tantalum surface at the melting temperature of niobium for various specimen configurations and heating rates.

Malter and Langmuir[10]. Values of ϵ_λ obtained from these functions were then used in Eq. (5) to convert the measured radiance temperatures for each specimen into true temperatures.

3.2. Melting Period Duration

The (true) temperatures for each specimen were fitted by the least squares method with a linear function of time for the melting period and to quadratic functions of time for the premelting and postmelting periods. The times t_1 and t_2 were determined for each specimen by the intersections of the quadratic functions with the linear function of time. For the nine specimens reported on herein, the duration of the melting period $(t_2 - t_1)$ ranged from about 55 ms for the most rapid experiments to about 120 ms for the slowest.

3.3. Heat Loss Corrections

The heat lost by radiation from the specimen surface is determined by means of the Stefan-Boltzmann equation,

$$P_r = \epsilon \sigma A_s (T^4 - T_0^4), \tag{6}$$

where ϵ is the hemispherical total emittance of the composite specimen, σ is the Stefan-Boltzmann constant (5.67032×10^{-8} W·m^{-2} · K^{-4}), A_s is the

surface area of the effective specimen (m^2), and T_0 is room temperature (296 K in our case). Consideration of the power balance for the specimen during the heating and initial free radiative cooling periods yields the following expression for ϵ (see ref. [6]):

$$\epsilon = \frac{EI}{\sigma A_s(T^4 - T_0^4)} \frac{(dT/dt)_c}{(dT/dt)_c - (dT/dt)_h} \tag{7}$$

where $(dT/dt)_h$ and $(dT/dt)_c$ are the heating and cooling rates (i.e., the slopes of the temperature-time functions fitted to the data by the least-squares method), respectively.

Calculations of ϵ from the data on Ta–Nb–Ta specimens, however, did not yield meaningful results, probably because of the development of undesirable temperature gradients during rapid cooling of the solid–liquid–solid composite under conditions of zero input power; this would affect the computed values of ϵ since Eq. (7) is rather sensitive to the slopes of the derived temperature-time functions.

Consequently, pulse heating experiments were carried out on Ta–Ta–Ta composite specimens with relative dimensions 5-10-5 and 10-10-10. The true temperatures of the specimens were determined from the measured radiance temperatures by means of the ϵ_λ data of Sec. 3.1; the (true) temperatures were fitted by the least-squares method to quadratic functions of time.The heating and cooling rates were computed for temperatures taken at equally spaced times along the heating curve. The voltage and current were calculated at the corresponding instants. Emittance was then computed for each temperature taken by means of Eq. (7). The emittances thus obtained were averaged for each experiment; the average ϵ was related to the average of the temperatures taken.

The average values of ϵ obtained from experiments in three pyrometer temperature ranges are presented as a function of temperature in Fig. 7. At 2750 K, the value of ϵ for the tantalum-5 surfaces is 0.325, which is about 2% lower than the value 0.332 for the tantalum-10 surfaces.

The fraction of the imparted energy, W_i, thermally radiated by each Ta–Nb–Ta specimen during the melting, was then computed by evaluating the time integral of Eq. (6); the values of ϵ used in the calculation were those obtained above for the Ta-5 and Ta-10 surfaces. The radiation losses ranged from about 10% of W_i for the fastest experiments to about 24% of W_i for the slowest.

A fraction of W_i was also absorbed by metal A (tantalum in the present case) as indicated by a slope in the melting plateau (see Table III). For the

nine specimens studied, the corresponding temperature rises during the melting period varied from about 1 to 14 K. The power absorbed by n_A moles of material A in raising its temperature dT during time interval dt is given by

$$P_A = n_A c_p \left(\frac{dT}{dt}\right)_A \tag{8}$$

where c_p is the heat capacity of A. The values of c_p for tantalum, used in the computations of P_A, were obtained from measurements by Cezairliyan et al. [11]. The fraction of W_i absorbed by A was obtained from the time integral of P_A during the melting period and was found to vary between about 0.1 and 1.5% of W_i.

3.4. Heat of Fusion

Heat of fusion of niobium was obtained with the use of Eq. (2) from the data on each composite specimen. The pertinent results are summarized in Table IV.

The average of nine values of the heat of fusion of niobium is 31.5 $kJ \cdot mol^{-1}$, with an average absolute deviation from the mean of 0.6 $kJ \cdot mol^{-1}$, and a maximum absolute deviation from the mean of 1.1 $kJ \cdot mol^{-1}$. In Fig. 8, the percentage deviation of the individual results from the mean value of the heat of fusion is given as a function of the rate of energy absorption by the niobium (a measure of the speed of the experiment).

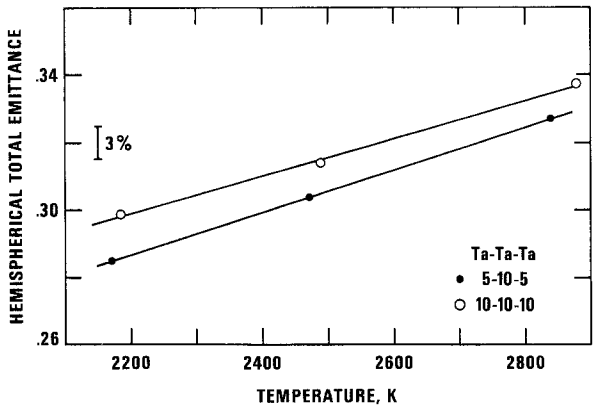

Fig. 7. Hemipherical total emittance for the tantalum-5 and tantalum-10 surfaces.

Table IV. Experimental Results on the Heat of Fusion of Niobium

Specimen number	Relative thickness[a] Ta–Nb–Ta	Effective mass of Nb[b] (g)	Melting time[c] (ms)	Energy imparted to specimen W_i (J)	Fraction of W_i radiated (%)	Fraction of W_i absorbed by Ta (%)	Fraction of W_i absorbed by Nb (%)	Rate of energy absorption by Nb ($kJ \cdot mol^{-1} \cdot s^{-1}$)	Heat of fusion ($kJ \cdot mol^{-1}$)
1	5-10-5	0.340	103.7	148.6	24.1	0.1	75.8	297	30.8
2	5-10-5	0.340	110.3	155.8	24.4	0.2	75.3	291	32.1
3	5-15-5	0.498	113.8	209.7	19.1	0.1	80.8	278	31.6
4	5-15-5	0.500	119.2	210.5	20.0	0.2	79.7	262	31.2
5	5-15-5	0.498	86.9	196.7	15.6	0.1	84.3	356	30.9
6	5-15-5	0.500	54.9	188.5	10.4	0.3	89.3	570	31.3
7	10-10-10	0.342	63.9	146.1	16.5	2.0	81.5	506	32.3
8	10-15-10	0.502	72.1	198.3	13.9	1.6	84.5	430	31.0
9	10-15-10	0.502	77.7	209.8	14.2	1.8	84.0	420	32.6

[a]Also indicates the nominal thicknesses in units of 10^{-3} in for the Ta and Nb strips used in the composite specimens.
[b]Determined from measurements of thickness of the Nb strips, the dimensions, and total mass of the composite specimen.
[c]Determined from the intersections, for the temperature-time function, of a linear least-squares fit to the melting plateau and quadratic least-squares fits to the temperatures before and after melting.

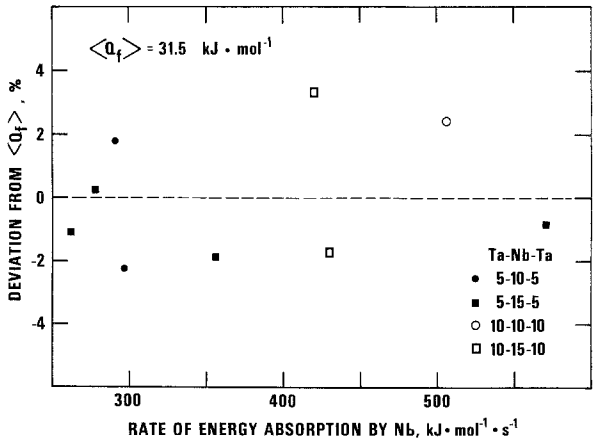

Fig. 8. Deviation of the heat of fusion results from the mean value $\langle Q_f \rangle$ as obtained for different specimen configurations at various rates of energy absorption by niobium.

3.5. Electrical Resistivity

The electrical resistance of a composite specimen as shown in Fig. 1 can be viewed as the net effect of two resistances in parallel: R_B, the resistance of the metallic strip under study, and R_A, the resistance of the outer two metallic strips. Therefore, it can be shown that the resistivity of metal B is given by

$$\rho_B = \rho_A \frac{C_B R_M}{\rho_A L - C_A R_M} \tag{9}$$

where ρ_A is the resistivity of metal A, R_M is the resistance determined by measurements of potential difference across the voltage probes and current through the specimen, L is the distance between voltage probes, and C_B and C_A are the total cross-sectional areas of strips B and A, respectively.

Resistivity values for niobium at temperatures between 2400 and 2900 K were obtained by means of Eq. (9), based on the resistivity of tantalum reported by Cezairliyan et al. [11]; results obtained from measurements on specimen 2 are presented in Fig. 9. The electrical resistivity of solid niobium (ρ_s) and of liquid niobium (ρ_L), at the melting point, were determined by means of least-squares fits to the computed resistivities for each Ta–Nb–Ta specimen before and after melting. Table V gives the values of ρ_s and ρ_L obtained from measurements on eight composite specimens. The mean value of the resistivity ratio ρ_L/ρ_s is 1.119, with an average absolute deviation from the mean of 0.004 and a maximum absolute deviation from the mean of 0.011.

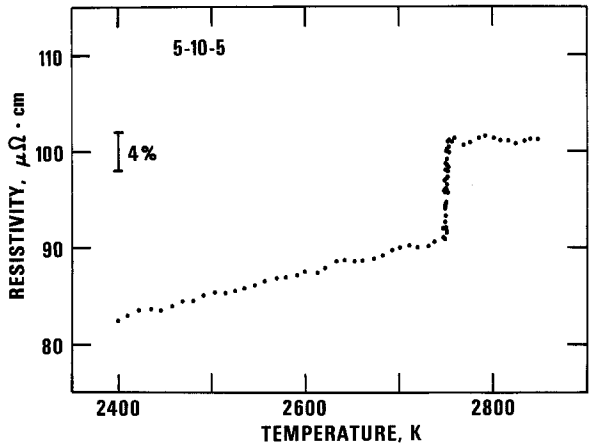

Fig. 9. Variation of electrical resistivity as a function of temperature near and at the melting temperature of niobium (Ta–Nb–Ta specimen with a relative thickness of 5-10-5).

In addition, the resistivity values of solid niobium obtained from all eight specimens were fitted by the least-squares method to a single function of temperature, yielding (standard deviation = 0.6%),

$$\rho = -19.24 + 5.941 \times 10^{-2}\, T - 7.190 \times 10^{-6}\, T^2 \tag{10}$$

for $2400 < T < 2750$, where T is in K and ρ is in $\mu\Omega \cdot$ cm. The corresponding fit of the resistivity values of liquid niobium yields (standard deviation = 1.0%)

$$\rho = 100.5\ \mu\Omega \cdot \text{cm} \tag{11}$$

for $2750 < T < 2900$.

3.6. Estimate of Errors

The methods of estimating errors in the measured quantities (temperature, voltage, and current) have been discussed at length in an earlier publication [6] on experiments involving tubular specimens fabricated from one material. In this paper, we consider only the specific items in the error analysis that differ from those in the earlier publication.

It is significant to note in Fig. 8 that the value obtained for the heat of fusion does not seem to depend on the speed of the experiment nor on the thickness combination used for the sandwich specimens. This suggests that

Table V. Experimental Results on the Electrical Resistivity of Niobium at its Melting Temperature

Specimen number	Relative thickness[a] Ta–Nb–Ta	Resistivity of solid Nb at the melting temp.		Resistivity of liquid Nb at the melting temp.		Resistivity ratio ρ_L/ρ_s
		ρ_s[b] ($\mu\Omega \cdot$ cm)	Std. dev.[c] ($\mu\Omega \cdot$ cm)	ρ_L[b] ($\mu\Omega \cdot$ cm)	Std. dev.[c] ($\mu\Omega \cdot$ cm)	
1	5-10-5	90.0	0.2	100.6	0.2	1.118
2	5-10-5	90.7	0.2	100.1	0.3	1.114
3	5-15-5	89.3	0.3	100.0	0.3	1.120
4	5-15-5	89.8	0.2	100.6	0.3	1.120
6	5-15-5	88.9	0.2	99.4	0.2	1.119
7	10-10-10	90.5	0.3	102.3	0.4	1.130
8	10-15-10	89.3	0.2	99.2	0.3	1.110
9	10-15-10	89.4	0.3	100.3	0.3	1.122

[a]Also indicates the nominal thicknesses in units of 10^{-3} in for the Ta and Nb strips used in the composite specimens.

[b]Resistivity of solid (or liquid) Nb as obtained from a least-squares fit to the measured values of resistivity before (or after) melting.

[c]Represents the standard deviation of an individual resistivity value from the smooth resistivity versus temperature function obtained by the least-squares method.

the effect on our results for heat of fusion by temperature gradients and/or chemical reaction is small when compared with other sources of error.

In the present work, three major sources of error contribute to the uncertainty in the value for the heat of fusion. These arise in determining the radiative heat loss correction, the melting period duration, and the mass of niobium in the effective specimen. In our experiments, temperature measurements were used primarily to establish the duration of the melting period. Errors in the temperature measurements affect the value for heat of fusion only to the extent that they affect the result for hemispherical total emittance, which was used in determining the radiative heat loss correction.

The accuracy of the measured specimen temperature can be crudely estimated by comparing our values for normal spectral emittance of the tantalum surfaces at 2750 K with values reported in the literature for the same temperature and similar specimen conditions. Our average values at 653 nm, 0.404 and 0.412 for the tantalum-5 and tantalum-10 surfaces, respectively, compare favorably with the value 0.400 (at 650 nm) reported by Cezairliyan et al. [11] and the value 0.41 (at 650 nm) obtained from the work by Abbott [12]. This suggests that the error in our value for ϵ_λ is less than 4%, which would correspond to an uncertainty of about 10 K in temperature. An error of 10 K in temperature contributes only a 0.2% uncertainty to the values of hemispherical total emittance (ϵ).

The maximum inaccuracy of the values of ϵ determined by our experiments is estimated to be about 5%. From Table IV, it may be shown that the energy radiated by the composite specimen during the melting period ranges from about 12 to about 30% of the energy absorbed by the niobium. Therefore, the uncertainty in ϵ will contribute to the heat of fusion value a maximum error of 0.6% for the most rapid experiments, increasing to 1.5% for the slowest experiments.

The maximum uncertainty in determining the duration of the melting period is estimated to be about 1 ms. This corresponds to an error in the heat of fusion value of approximately 2% for the most rapid experiments, decreasing to about 1% for the slowest experiments.

The mass of niobium in the effective specimen was determined from measurements of thickness of the niobium strips, the dimensions, and total mass of the composite specimens prior to the experiments. The mass of a number of composite specimens was remeasured after the pulse heating experiments to check for possible loss of niobium during its liquid phase; no change in mass was detected. The maximum error in the value for the niobium mass, hence the error contribution to the heat of fusion, is estimated to be about 2% in the worst case (niobium-10 strips). Therefore, the maximum error (random plus systematic) from all sources in our reported value for the heat of fusion of niobium is estimated to be approximately 5%.

The maximum error in the reported resistivity values for niobium [Eq.

(10) and (11)] is estimated to be about twice the standard deviation of the least-squares approximation of the data, that is, about 1% for the resistivity values in the solid phase and 2% for the resistivity values in the liquid phase.

4. DISCUSSION

The earlier measurements by other investigators on the heat of fusion of niobium were carried out by means of either levitation calorimetry [1, 13] or by capacitor discharge techniques [14–16]; the latter methods are about three to four orders of magnitude faster than the pulse heating technique used in the present work. A comparison of the results reported in the literature with the result of our work is given in Table VI. It is interesting to note that the earlier values fall into two groups: those around 33 kJ·mol^{-1} and others around 28 kJ · mol^{-1}. However, the disagreement of nearly 20% is not the result of a bias toward a measurement technique, since values obtained by a given technique can be found in either group. The heat of fusion values reported by Margrave [1] and by Martynyuk et al. [15] are about 5% higher than our reported value of 31.5 kJ · mol^{-1}; this difference lies within the uncertainties in the experiments. However, the values of Sheindlin et al. [13], Savvatimskii [14], and Shaner et al. [16] are all about 12% lower than our result.

The values 31.5 kJ · mol^{-1} for the heat of fusion and 2750 K for the melting temperature yield a value of 11.4 J · mol^{-1} · K^{-1} for the entropy of fusion of niobium. This experimental value, as well as those for other refractory metals [1, 16], is considerably higher than the value 7.4 J · mol^{-1} · K^{-1} suggested by Gschneider [17] for body-centered-cubic metals.

Figure 10 compares the values of electrical resistivity for niobium near and at the melting temperature as reported in the literature. The agreement between our results for solid niobium and those obtained earlier by Cezairliyan [18] is remarkably good considering that the earlier measurements were

Table VI. Heats of Fusion of Niobium Reported in the Literature

Investigator	Ref.	Year	Heat of fusion (kJ · mol^{-1})	Technique
Margrave	1	1970	33.1	Levitation calorimetry
Sheindlin et al.	13	1972	27.6	Levitation calorimetry
Savvatimskii	14	1973	27.6	Pulse heating[a]
Martynyuk et al.	15	1975	33.0	Pulse heating[a]
Shaner et al.	16	1977	27.9	Pulse heating[a]
Present work			31.5	Pulse heating[b]

[a]Capacitor discharge technique yielding melting times in the range of about 10^{-4} to 10^{-6} s.
[b]Energy supplied by a battery bank yielding melting times in the range of about 10^{-1} to 10^{-2} s.

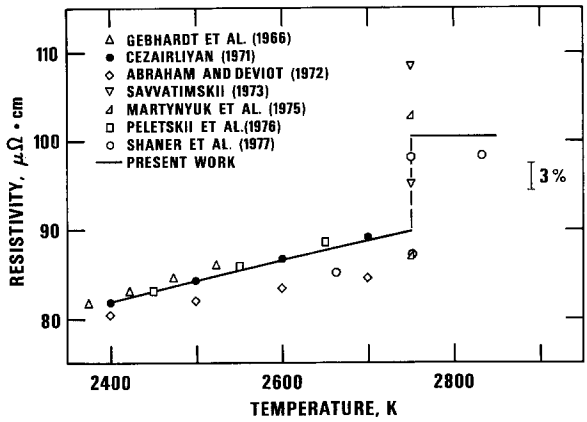

Fig. 10. Values of electrical resistivity near and at the melting temperature of niobium as reported in the literature. All data are based on the room temperature dimensions of the specimens.

made on tubular specimens, permitting true temperatures to be measured directly, whereas the present values were derived from measurements on metal sandwiches by subtracting out the tantalum resistivities and converting the measured radiance temperatures to true temperatures. This agreement tends to confirm the internal consistency of our procedure in obtaining thermophysical properties data from a metal sandwich. Also, it may be seen that our resistivity values lie within 1% of the results obtained by Gebhardt et al. [19] and by Peletskii et al. [20]. However, the results of Abraham and

Table VII. Electrical Resistivity[a] of Solid (ρ_s) and Liquid (ρ_L) Niobium at its Melting Temperature as Reported in the Literature

Investigator	Ref.	Year	Resistivity at the melting temp. ($\mu\Omega$ · cm)		Resistivity ratio
			ρ_s	ρ_L	ρ_L/ρ_s
Savvatimskii	14	1973	95.2	108.5	1.14
Martynyuk et al.	15	1975	86.9	102.7	1.18
Shaner et al.	16	1977	89[b]	101[b]	1.13
Present work			89.8	100.5	1.12

[a]All data except for those of ref. [16] are based on room temperature dimensions of the specimen.

[b]Corresponding values based on room temperature dimensions are $\rho_s = 87$, $\rho_L = 98$.

Deviot [21] are somewhat lower, the divergence approaching 4% at the melting temperature.

The change in resistivity during the solid-liquid transformation has been measured earlier by Savvatimskii [14], Martynyuk et al. [15], and by Shaner et al. [16], all using capacitor discharge techniques. The results are compared with our measurements in Table VII as well as Fig. 10. The disagreement among the different values is as large as 10%. Only the work by Shaner et al. extends far into the liquid region, beyond 4000 K; their data are systematically lower than our results by about 3% throughout the temperature range common to both experiments.

In conclusion, the results obtained in this investigation demonstrate the feasibility of using a subsecond pulse heating technique for measuring the heat of fusion and the electrical resistivity of refractory metals around their melting temperatures.

ACKNOWLEDGMENTS

This work was supported in part by the U.S. Air Force Office of Scientific Research. The authors express their appreciation to M. S. Morse for his help with the electronic instrumentation.

REFERENCES

1. J. L. Margrave, *High Temperatures-High Pressures* **2**:583 (1970).
2. V. Ya. Chekhovskoi, A. E. Sheindlin, and B. Ya. Berezin, *High Temperatures-High Pressures* **2**:301 (1970).
3. S. V. Lebedev, A. I. Savvatimskii, and Yu. B. Smirnov, *High Temperature* **9**:578 (1971).
4. J. W. Shaner, G. R. Gathers, and C. Minichino, *High Temperatures-High Pressures* **8**:425 (1976).
5. A. Cezairliyan, *J. Res. Natl. Bur. Stand. (U.S.A.)* **75C**:7 (1971).
6. A. Cezairliyan, M. S. Morse, H. A. Berman, and C. W. Beckett, *J. Res. Natl. Bur. Stand. (U.S.A.)* **74A**:65 (1970).
7. G. M. Foley, *Rev. Sci. Instr.* **41**:827 (1970).
8. International Practical Temperature Scale of 1968, *Metrologia* **5**:35 (1969).
9. A. Cezairliyan, *High Temperatures-High Pressures* **4**:453 (1972).
10. L. Malter and D. B. Langmuir, *Phys. Rev.* **55**:743 (1939).
11. A. Cezairliyan, J. L. McClure, and C. W. Beckett, *J. Res. Natl. Bur. Stand. (U.S.A.)* **75A**:1 (1971).
12. G. L. Abbott, WADD-TR-61-94, Pt. 3 (1963).
13. A. E. Sheindlin, B. Ya. Berezin, and V. Ya. Chekhovskoi, *High Temperatures-High Pressures* **4**:611 (1972).
14. A. I. Savvatimskii, *High Temperature* **11**:1057 (1973).
15. M. M. Martynyuk, I. Karimkhodzhaev, and V. I. Tsapkov, *Sov. Phys. Tech. Phys.* **19**:1458 (1975).
16. J. W. Shaner, G. R. Gathers, and W. M. Hogson, in *Proceedings of the Seventh Symposium on Thermophysical Properties,* A. Cezairliyan, ed. (ASME, New York, 1977), p. 896.

17. K. Gschneidner, in *Solid State Physics, Vol 16,* F. Seitz and D. Turnbull, eds. (Academic, New York, 1964), p. 275.
18. A. Cezairliyan, *J. Res. Natl. Bur. Stand. (U.S.A.)* **75A:**565 (1971).
19. E. Gebhardt, W. Durrschnable, and G. Horz, *J. Nucl. Mat.* **18:**119 (1966).
20. V. E. Peletskii, E. S. Amasovich, E. B. Zaretskii, and Ya. G. Sobol', *Russian Metallurgy,* No. 5, 44 (1976).
21. J. M. Abraham and B. Deviot, *J. Less-Common Metals* **29:**311 (1972).